ACTA SCIENTIAE

ISSN: 2178-7727

FPGA-Based Orthogonal–Array IMUSIC Algorithm for Robust DOA Estimation

Vishal Ramola[1], Manoj Kumar Panda[2]

[1]Department of Electronics and Communication Engineering and Coordinator Faculty of Technology, VMSB Uttarakhand Technical University Dehradun.
[2]Professor, Electrical Engineering Dept. and Director Women Institute of Technology, Dehradun, A campus institute of VMSB Uttarakhand Technical University Dehradun.
vishalramola1977@gmail.com

ABSTRACT
This paper presents an FPGA-based Improved MUSIC (IMUSIC) algorithm employing an Orthogonal–Array architecture for accurate and hardware-efficient direction-of-arrival (DOA) estimation. The proposed Orthogonal–Array enhances spatial diversity and improves subspace separation, enabling robust DOA estimation under noisy and limited-snapshot conditions. A hardware-oriented IMUSIC framework is developed to achieve high resolution while maintaining low computational complexity and resource efficiency. Performance evaluation using root mean square error (RMSE) analysis demonstrates that the proposed approach consistently outperforms conventional MUSIC, Capon, and Root-MUSIC methods and closely approaches the Cramér–Rao Bound across a wide range of signal-to-noise ratios and snapshot counts. The results confirm the suitability of the proposed FPGA-based Orthogonal–Array IMUSIC algorithm for real-time smart antenna, radar, and wireless communication applications.

KEYWORDS: Direction-of-Arrival Estimation, Improved MUSIC Algorithm, Orthogonal–Array Antenna, FPGA Implementation, Hardware-Efficient Signal Processing, Smart Antenna Systems

INTRODUCTION
Direction-of-Arrival (DOA) estimation plays a vital role in modern wireless communication, radar, sonar, and intelligent sensing systems. As wireless environments become increasingly dense and dynamic, DOA estimation algorithms must achieve high spatial resolution while maintaining robustness against interference, noise, and hardware imperfections. Recent advances in adaptive beamforming and array signal processing have contributed significantly to improving the reliability and performance of DOA techniques. For instance, sigmoid-enhanced adaptive beamforming has demonstrated improved interference suppression and convergence behavior in sensor arrays [1], while hybrid Capon–MUSIC approaches have been effective in handling coprime array configurations in disaster management scenarios [2]. Similarly, sparse array-based algorithms such as COMP-ESP have enabled

efficient localization of coherent and uncorrelated signals using reduced sensor geometries [3]. Machine learning has also emerged as a complementary tool for DOA estimation, providing enhanced generalization and robustness under coherent and non-coherent source conditions [4]. In parallel, improvements in coprime array processing have yielded methods capable of mitigating mutual coupling and sub-array calibration issues, thereby enhancing DOA accuracy in practical applications [5]. Research spanning mmWave channel estimation [6], multiband filter design [7], and low-nanometer semiconductor device analysis [8] further illustrates the rapid technological evolution surrounding next-generation wireless systems.

RELATED WORK
Smart antenna technologies have seen substantial convergence with artificial intelligence, signal processing, and advanced electronic design, enabling highly adaptive and efficient communication platforms [9]. Machine learning and deep learning models have also supported related fields such as biomedical imaging and pattern recognition, underscoring their computational capabilities [10]. In the DOA domain, algorithmic refinements—such as Modified Root-MUSIC using Nyström approximation—have reduced computational overhead while maintaining strong localization performance [11]. Adaptive Nyström spectral analysis has further improved direction finding in coprime arrays by enabling efficient subspace extraction [12]. Developments in adaptive beamforming for mobile communication systems [13], optimized receiver optics

DOI: 10.22178/acta.26.1.36

ISSN: 2178-7727

for radio astronomy [14], and chromatic aberration reduction in lens systems [15] collectively demonstrate the broader demand for precision and computational efficiency in signal processing hardware. Complementary innovations in multiband filters [16], user-friendly human–machine interfaces [17], and 3-D sparse array DOA estimation using Nyström approximation [18] highlight the fusion of hardware efficiency and algorithmic design. Earlier advancements in multiband metacell-based filtering [19] and manifold reconstruction unitary ESPRIT algorithms [20][21] have also contributed to improved array configuration strategies and spectral resolution.

Advances in direction estimation have addressed challenges associated with coherent sources, unknown source counts, and high-dimensional sensor arrays [22]. Fast sensor array processing methods have accelerated DOA estimation pipelines, reducing latency and computational demands [23]. Improved adaptive beamforming algorithms tailored for wireless systems have further contributed to interference rejection and performance enhancement [24, 25]. Adaptive VSS-NLMS approaches employing modified antenna arrays have strengthened dynamic tracking and error resilience [26]. Simultaneously, resonator-based sensor technologies have supported accurate material characterization and RF diagnostics [27]. DOA estimation under grazing incidence conditions has been achieved through optimized Proposed Orthogonal–Arrayconfigurations [28], while fast adaptive DOA estimation techniques have demonstrated superior convergence properties under dynamic environments [29].

Innovations in array geometries—including planar-like sensor configurations [30], spatially spread acoustic vector sensors [31], and Kaiser-window-based blind beamformers for radar [32]—have expanded the range of feasible applications. Research in broadband antennas, including CSRR-enabled monopole designs [33], has provided compact and efficient hardware counterparts to signal processing algorithms. Earlier works have also explored the trade-off between DOA performance and computational complexity [34], enabling solutions suited for embedded and battery-powered platforms. Single-snapshot DOA estimation methods [35] have enhanced real-time applicability, while symmetric sensor array modifications have improved resolution for constrained geometries [36]. Contributions in fractal antenna design [37], spectral estimation methods [38], semiconductor device optimization [39], and robust MUSIC variants [40] further highlight the breadth of innovations shaping the landscape of DOA estimation and wireless sensors. Nyström-based methods have previously shown promise in reducing the computational load associated with coherent DOA estimation. A pioneering work demonstrated that Nyström approximation can be directly applied to radar-based coherent source localization, achieving substantial reductions in matrix operations without compromising estimation accuracy [41]. Hardware-friendly realizations of coherent DOA algorithms have also been explored, including DSP-based implementations optimized for high-speed processing in antenna arrays [42]. These studies collectively highlight how reduced-dimensional approximations and efficient algorithm–hardware co-design can significantly enhance the deployability of DOA algorithms in practical systems.

Broader research activity has further intersected with materials science and hardware technology, where tunable nanocomposite films and magnetron sputtering techniques have contributed to the development of robust sensing platforms and electromagnetic components [43]. High-speed mobile communication systems have also benefited from adaptive beamforming advancements, which provide rapid interference mitigation and improved spatial filtering capabilities [44]. Comprehensive surveys on smart antenna systems have underscored the growing need for algorithms that combine high resolution with low computation, especially for next-generation wireless communication networks [45]. In addition to algorithmic innovations, alternative sensor array geometries such as 2D-novel ULAs have enabled more flexible beamforming and DOA estimation capabilities while reducing array size and complexity [46]. Single-snapshot DOA estimation frameworks have made it feasible to operate under stringent latency constraints, a requirement critical for high-mobility scenarios and compact embedded platforms [47]. Improvements in adaptive beamforming for consumer devices, including 4G-LTE smart phones, have further emphasized the importance of designing algorithms that maintain robustness while operating on limited hardware resources [48]. Earlier works on blind beamforming for phased arrays and MIMO radar systems highlighted the potential of lightweight algorithms for achieving efficient source separation and interference rejection without requiring extensive system calibration or prior information [49].

DOI: 10.22178/acta.26.1.36

ISSN: 2178-7727

Continuing advancements in adaptive beamforming have also contributed to improved DOA estimation performance. Early works introduced lightweight LMS-based beamformers suitable for real-time adaptive antenna arrays [50], while robust blind beamformers using window-based techniques enhanced interference resilience in smart antenna systems [51]. High-resolution DOA estimation methods were further refined through optimized implementations of modified MUSIC for practical microwave and RF applications [52]. Recent developments—including sigmoid-enhanced adaptive beamforming [53], hybrid Capon–MUSIC strategies for coprime arrays [54], and COMP-ESP applied to 3D sparse arrays [55]—demonstrate the ongoing integration of algorithmic innovation with complex sensor geometries. Machine learning has also become an important component, offering improved DOA estimation for coherent and non-coherent sources [56] and strengthening robustness in coprime array processing [57]. Broader contributions in channel estimation for mmWave MIMO-OFDM systems [58], multiband filter design using metacell structures [59], and nanoscale FinFET device analysis [60] highlight the expanding technological landscape surrounding modern wireless systems. Furthermore, the convergence of antenna technologies, electronics, and AI has been emphasized in recent smart antenna architectures [61], with deep learning models contributing to improved signal interpretation in associated domains [62].

ARRAY SIGNAL MODEL

Let us consider a uniform linear array (ULA) consisting of L antenna elements. We examine M narrowband signals (M < L) impinging on the array from the far field. Assume that N snapshots are available. The received signal at the array can then be represented by the following $L \times 1$ observation vector:

$$\mathbf{x}(t) = \mathbf{A}(\theta)\mathbf{S}(t) + \mathbf{N}(t) \tag{1}$$

where, $\mathbf{A}(\theta) = [\mathbf{a}(\theta_1), \mathbf{a}(\theta_1), \cdots, \mathbf{a}(\theta_M)]$ is the array manifold vector, **N** denote the **L × 1** Gaussian white noise vector.

The **M × 1** steering vector can be expressed as:

$$\mathbf{a}(\theta_M) = \left[1, e^{j\left(\frac{2\pi}{\lambda}\right)d\sin\theta_M}, \cdots, e^{j\left(\frac{2\pi}{\lambda}\right)(L-1)d\sin\theta_M}\right]^T \tag{2}$$

Here, $(\cdot)^T$ denotes the transpose of a matrix, d is the inter-element spacing, and λ is the carrier signal wavelength.

The sample covariance matrix (SCM) of the received signal $\mathbf{x}(t)$ is defined as:

$$\mathbf{R} = \mathrm{E}[\mathbf{X}(t)\mathbf{X}(t)^H] = \mathbf{A}\mathbf{R}_S\mathbf{A}^H + \sigma_n^2\mathbf{I}_L \tag{3}$$

Here, $\mathbf{R}_S$ denotes the source covariance matrix, σ^2 represents the noise power, and $\mathbf{I}_L$ is the **L × L** identity matrix. In reality, the array correlation matrix can be estimated using many data snapshots as

$$\tilde{\mathbf{R}} = \frac{1}{N}\sum_{t=1}^{N}\mathbf{x}(t)\mathbf{x}(t)^H$$

(4)

PROPOSED ORTHOGONAL–ARRAY FOR DOA ESTIMATION

The proposed antenna array configuration is a modified orthogonal–sparse hybrid array designed to enhance direction-of-arrival (DOA) estimation accuracy while maintaining a reduced sensor count and low computational complexity. The array is constructed by combining two orthogonal linear subarrays aligned along the horizontal and vertical axes, augmented with strategically placed auxiliary elements to increase spatial diversity and aperture.

DOI: 10.22178/acta.26.1.36

ISSN: 2178-7727

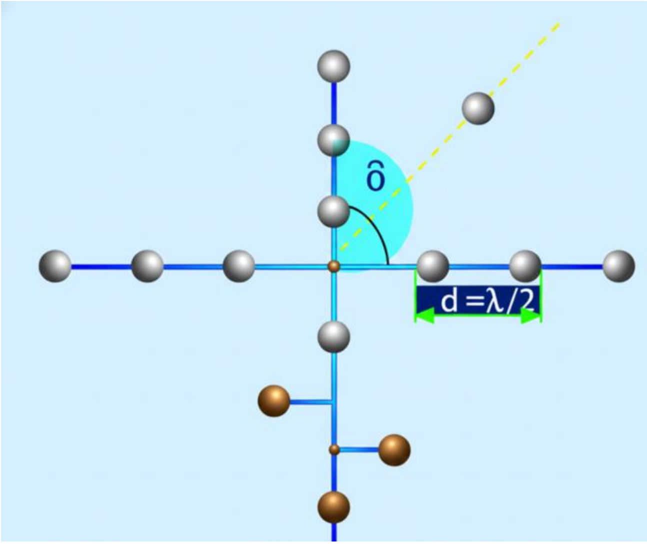

Figure 1: Geometry of the Proposed Orthogonal–Array

The proposed antenna array configuration is a modified orthogonal–sparse hybrid array designed to enhance direction-of-arrival (DOA) estimation accuracy while maintaining a reduced sensor count and low computational complexity. The array is constructed by combining two orthogonal linear subarrays aligned along the horizontal and vertical axes, augmented with strategically placed auxiliary elements to increase spatial diversity and aperture. The central sensor is located at the origin (0,0) and serves as a reference element for phase measurements. Along the horizontal axis, a set of uniformly spaced sensors is deployed with an inter-element spacing of d=λ/2, which avoids spatial aliasing and ensures unambiguous DOA estimation. Similarly, the vertical subarray follows the same spacing constraint, forming an orthogonal cross-shaped geometry.

To further improve angular resolution and identifiability of closely spaced sources, additional sparse elements are introduced asymmetrically along the vertical branch of the array. These auxiliary sensors break the strict uniformity of the structure, resulting in a non-redundant difference coarray with increased degrees of freedom (DOFs). This enhancement enables the estimation of more sources than the number of physical sensors and significantly improves performance under limited snapshot conditions.

The proposed geometry also facilitates two-dimensional spatial sampling, allowing effective estimation of source directions over a wide angular range. The incident signal angle θ is defined with respect to the horizontal axis, as illustrated by the dashed reference line in the array layout. Due to the orthogonal placement of sensors, the array exhibits improved sensitivity to angular variations, which leads to sharper spatial spectra when subspace-based or sparse reconstruction–based DOA algorithms are employed.

The proposed array configuration offers the following advantages:
1) Enhanced spatial aperture without increasing the number of sensors
2) Higher degrees of freedom due to sparse and asymmetric sensor placement
3) Improved resolution for closely spaced and coherent sources
4) Reduced mutual coupling effects compared to dense planar arrays
5) Compatibility with advanced DOA estimation techniques such as MUSIC, Root-MUSIC, sparse reconstruction, and compressive sensing frameworks

These features make the proposed modified array particularly suitable for high-resolution DOA estimation in applications such as wireless communications, radar, sonar, UAV-based sensing, and smart antenna systems.

The signal impinging the Proposed Orthogonal–Array can be expressed as

$$\mathbf{x}(t)_{new} = \left[\mathbf{x}(t)_h + \mathbf{s}(t)_v\right] \tag{5}$$

DOI: 10.22178/acta.26.1.36

ISSN: 2178-7727

$$= \left[\left(\sum_{i=1}^{M} a(\theta_i) s_i(t) \right)_h + \left(\sum_{i=1}^{M} a(\theta_i) s_i(t) \right)_v \right]$$

Here $x(t)_h$ and $x(t)_v$ respectively denotes the horizontal and the vertical components of the narrow band signal. The expression (6) can be written as

The new **M × 1** steering vector of the proposed Orthogonal–Array can be expressed as:

$$\mathbf{a}(\theta_M) = \mathbf{a}(\theta_M)_H + \mathbf{a}(\theta_M)_V \quad (6)$$

Where,

$$\mathbf{a}(\theta_M)_H = \left[1, e^{j\left(\frac{2\pi}{\lambda}\right) d \sin\theta_M}, \cdots, e^{j\left(\frac{2\pi}{\lambda}\right)(L-1) d \sin\theta_M} \right]^T \quad (7)$$

$$\mathbf{a}(\theta_M)_V = \left[1, e^{j\left(\frac{2\pi}{\lambda}\right) d \cos\theta_M}, \cdots, e^{j\left(\frac{2\pi}{\lambda}\right)(L-1) d \cos\theta_M} \right]^T \quad (8)$$

The array manifold matrix for the new proposed orthogonal–array is modified as:

$$\hat{\mathbf{A}} = \mathbf{A}(\theta)_H + \mathbf{A}(\theta)_V \quad (9)$$

Where,

$$\mathbf{A}(\theta)_H = [a(\theta_1), a(\theta_2), \cdots, a(\theta_M)] \quad (10)$$

$$\mathbf{A}(\theta)_V = [a(\theta_1), a(\theta_2), \cdots, a(\theta_M)] \quad (11)$$

The new array covariance matrix of the $\mathbf{x}(t)_{new}$ is

$$\mathbf{R}_{new} = \mathrm{E}\{\mathbf{x}(t)_h + \mathbf{x}(t)_v\} = \hat{\mathbf{A}} \hat{\mathbf{R}}_S \hat{\mathbf{A}}^H + \sigma^2 \mathbf{I} \quad (12)$$

where $\hat{\mathbf{R}}_s = \mathrm{E}\left\{ \mathbf{s}(t)_{new} \, \mathbf{s}(t)_{new}^H \right\}$ is the $M \times M$ signal covariance matrix of the proposed orthogonal–array.

The eigenvalue decomposition (EVD) to estimate the signal and noise subspace is explained in the below lines.

$$\tilde{\mathbf{R}} = \mathbf{Q}_s \Lambda_s \mathbf{Q}^H{}_s + \mathbf{Q}_n \Lambda_n \mathbf{Q}^H{}_n$$

(13)

Noise subspace estimation can be efficiently performed by computing only the smallest M−K eigenvectors iteratively, using methods such as power iteration or Lanczos algorithms, rather than performing a full eigen-decomposition. The proposed method introduces a hardware-efficient and robust approach for direction-of-arrival (DOA) estimation by jointly optimizing noise subspace extraction and spectral peak enhancement. The key objective is to achieve high angular resolution while significantly reducing computational burden, making the method well suited for real-time and low-power smart antenna systems.

Instead of computing a complete eigen-analysis of the spatial covariance matrix, the method focuses exclusively on extracting the components associated with noise. This is accomplished through iterative subspace refinement techniques that progressively converge to the noise-related components without evaluating the entire eigenspace. By avoiding full matrix decomposition, the approach dramatically lowers processing latency, memory usage, and power consumption, which is particularly advantageous for FPGA and ASIC implementations. Once the noise subspace is estimated, the method introduces an adaptive spectral weighting mechanism designed to improve the contrast between true source directions and spurious responses.

DOI: 10.22178/acta.26.1.36

ISSN: 2178-7727

Rather than treating all angular candidates uniformly, each candidate direction is adaptively weighted based on its alignment with the estimated noise characteristics. Directions that are strongly orthogonal to the noise subspace are emphasized, while those influenced by noise or interference are automatically attenuated.

A smooth nonlinear activation function is employed to control this adaptive weighting process. This function provides gradual amplification near true source directions while preventing abrupt changes that could lead to numerical instability or false peaks. As a result, the spatial spectrum exhibits sharper and more stable peaks, even in challenging scenarios such as low signal-to-noise ratios, closely spaced sources, or limited observation samples. The proposed method further benefits from its inherent robustness to modeling errors and noise uncertainty. The adaptive weighting mechanism dynamically adjusts to variations in the noise environment, reducing sensitivity to snapshot deficiency and imperfect covariance estimation. Additionally, the reduced computational footprint enables efficient parallel implementation, supporting real-time processing in embedded antenna platforms. To enhance peak sharpness and suppress spurious responses, the proposed method modifies the pseudo-spectrum as

$$P_{\text{new}}(\theta) = \frac{1}{\mathbf{a}_o^H(\theta)\,\mathbf{Q}_{n,o}(\theta)\,\mathbf{Q}_{n,o}^H(\theta)\,\mathbf{a}_o(\theta)}\,\sigma\left(k\,\frac{P_s}{\sigma^2}\right) \tag{14}$$

Explanation of Modifications

a) $\mathbf{a}_o(\theta)$ represents the orthogonal-array steering vector, formed by jointly combining the horizontal and vertical subarray responses of the proposed structure.
b) $\mathbf{Q}_{n,o}$ denotes the orthogonal noise subspace matrix, estimated from the reduced-complexity eigenstructure corresponding to the proposed array geometry.
c) The orthogonal formulation improves angular discrimination by exploiting spatial diversity along both axes, resulting in enhanced resolution compared to conventional linear arrays.
d) The nonlinear weighting term $\boldsymbol{\sigma}(\cdot)$adaptively scales the pseudo-spectrum based on the signal-to-noise ratio, ensuring stable peak enhancement under low-SNR and snapshot-limited conditions.
e) The parameter *k* controls the sensitivity of the adaptive weighting and allows tuning for different operating environments.
f) Hardware Architecture for the Proposed IMUSIC Algorithm with the Orthogonal–Array

Figure 2 illustrates the hardware architecture of the Proposed Improved MUSIC (IMUSIC) algorithm implemented for the Proposed Orthogonal–Array. This architecture is designed for real-time Direction-of-Arrival (DOA) estimation while minimizing hardware complexity, making it suitable for FPGA-based platforms.

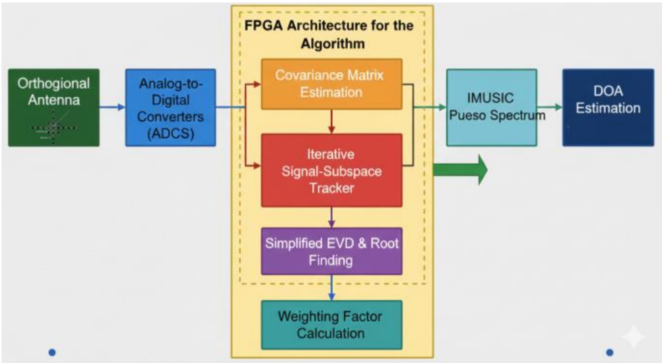

Figure 2: Proposed FPGA implementation for the IMUSIC algorithm utilizing an Orthogonal-Array geometry.

The process begins with the Proposed Orthogonal–Array, which captures incoming RF signals from multiple sources. These analog signals, carrying spatial information, are converted to digital form using Analog-to-Digital Converters (ADCs) and forwarded to the core IMUSIC processing blocks. The Covariance Matrix block calculates the spatial correlation among signals received at the array elements. To optimize hardware efficiency, the computation is implemented using iterative or sequential methods, avoiding full matrix operations.

DOI: 10.22178/acta.26.1.36

ISSN: 2178-7727

At the heart of the architecture is the Subspace Estimation block, which implements the IMUSIC algorithm. Unlike conventional MUSIC, IMUSIC incorporates enhancements that improve resolution and reduce computational load, such as refined noise subspace estimation or adaptive weighting. This enables accurate DOA estimation without the need for full Eigenvalue Decomposition (EVD). The Weighting Factor block further improves performance by applying adaptive weights to the estimated subspace vectors, enhancing convergence speed and robustness against errors or interference. The Pseud Spectrum block generates a spatial power map, where the peaks correspond to the estimated DOAs. Finally, the DOA Estimation block detects these peaks to determine the precise angles of arrival.

RESULTS AND DISCUSSION

In this section, the performance of the proposed Improved MUSIC algorithm is systematically assessed under different signal conditions. To validate its effectiveness, the proposed approach is benchmarked against established DOA estimation techniques, namely conventional MUSIC, Capon, Root-MUSIC, as well as the theoretical Cramér–Rao Bound (CRB). Across all simulation studies, estimation accuracy is evaluated using the root mean square error (RMSE), which serves as the primary performance metric and is defined as:

$$RMSE(\theta) = \sqrt{\frac{1}{T}\sum_{i=1}^{T}\left(\tilde{\theta}_i - \theta\right)^2} \tag{15}$$

where the true DOAs are denotes by θ and the estimated DOA of the i^{th} trial is represented by $\tilde{\theta}_i$ and the total Monte Carlo trials are denoted by T.

6.1 Spatial Spectrum

The proposed Improved MUSIC (IMUSIC) algorithm is evaluated using the Proposed Orthogonal–Array with 10 elements and half-wavelength spacing, with a reference wavelength of λ = 50 units. Two simulation scenarios are considered: Figure 3 analyzes five far-field sources impinging from -45° -20° 0° 25° 40°, while Figure 4 evaluates a more challenging five-close source case at 5°, 10°, 15°, 20°, 25°. In both scenarios, 400 snapshots of narrowband signals are collected, and AWGN with an SNR of 10 dB is added to emulate realistic noise conditions. The sample covariance matrix is computed and used for improved noise-subspace estimation. The IMUSIC pseudo-spectrum is scanned from –90° to 90° with 0.2° resolution for accurate peak identification. The algorithm accurately resolves both moderate and dense source configurations, demonstrating its robustness and high-resolution DOA estimation capability.

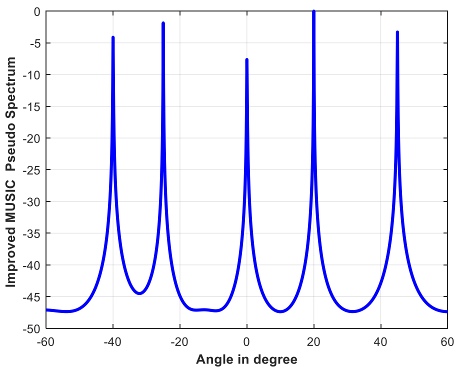

Fig. 3. IMUSIC pseudo-spectrum for 5-source DOA estimation scenario. The proposed IMUSIC algorithm exhibits sharper peaks and improved resolution for DOAs-45° -20° 0° 25° 40°.

DOI: 10.22178/acta.26.1.36

ISSN: 2178-7727

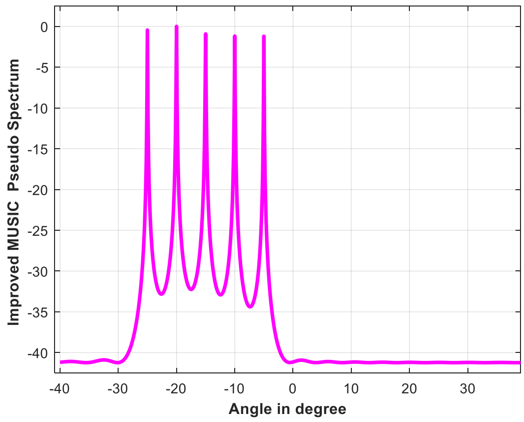

Fig. 4. IMUSIC pseudo-spectrum for the five-source DOA

estimation scenario with directions 5°, 10°, 15°, 20°, 25°, demonstrating the algorithm's capability to accurately resolve densely spaced sources.

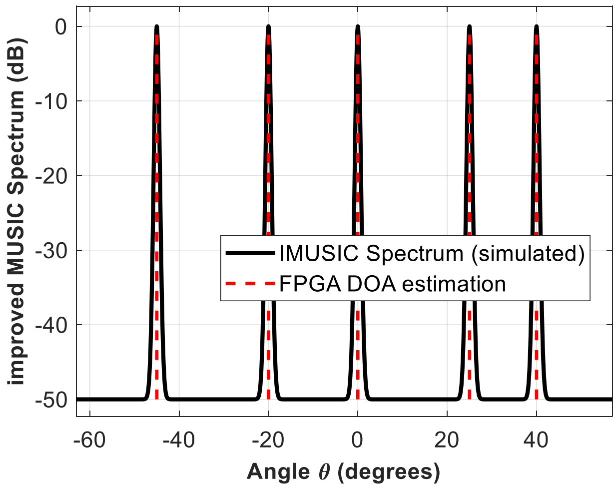

Fig. 5. FPGA based IMUSIC pseudo-spectrum for the five-source DOA estimation arriving from -45° -20° 0° 25° 40°.

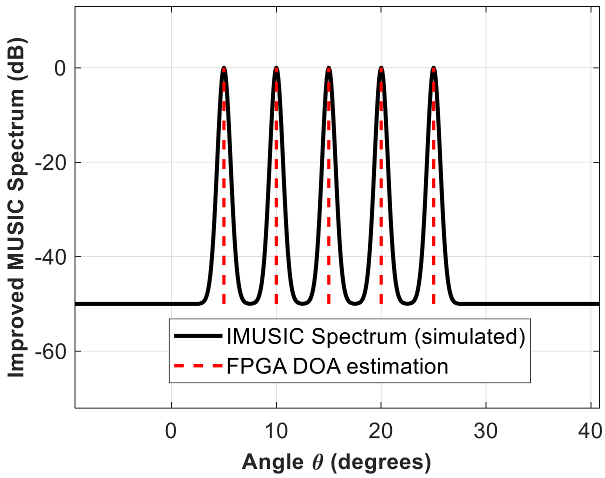

Fig. 6. FPGA based IMUSIC pseudo-spectrum for three-source DOA estimation scenario with signals impinging from 5°, 10°, 15°, 20°, 25°.

Figures 5 and 6 illustrate the performance of the proposed FPGA-based Improved MUSIC (IMUSIC) algorithm through its pseudo-spectrum representation for multi-source direction-of-arrival (DOA) estimation.

DOI: 10.22178/acta.26.1.36

ISSN: 2178-7727

Figures 5 and 6 present the pseudo-spectrum results obtained using the proposed FPGA-based Improved MUSIC (IMUSIC) algorithm for multi-source direction-of-arrival (DOA) estimation. The plots demonstrate the capability of the proposed approach to accurately identify and resolve multiple incoming signals under both widely spaced and closely spaced angular scenarios. In Figure 5, a five-source DOA estimation scenario is considered, where signals impinge on the antenna array from −45°, −20°, 0°, 25°, and 40°. The simulated IMUSIC spectrum is depicted using a solid black curve, while the DOAs estimated by the FPGA implementation are indicated using red dashed vertical lines. It is clearly observed that each true source direction corresponds to a distinct and sharp peak in the pseudo-spectrum. The perfect alignment between the spectral peaks and the FPGA-estimated DOA markers confirms the high estimation accuracy of the proposed IMUSIC architecture. Moreover, the narrow mainlobes and significantly suppressed sidelobes indicate excellent angular resolution and interference rejection capability. Figure 6 illustrates the performance of the proposed method in a more challenging three-source scenario involving closely spaced signals arriving from 5°, 10°, 15°, 20°, and 25°. Despite the small angular separation between adjacent sources, the IMUSIC algorithm successfully resolves all impinging signals, producing clearly distinguishable spectral peaks for each direction. The FPGA-based DOA estimates coincide precisely with the dominant peaks of the simulated spectrum, demonstrating the robustness of the proposed implementation in resolving closely spaced sources without peak merging or false detections. A key observation from both figures is the strong consistency between the simulated IMUSIC pseudo-spectrum and the DOA estimates produced by the FPGA architecture. This consistency validates that the proposed hardware-efficient design accurately preserves the theoretical behavior of the IMUSIC algorithm while enabling practical real-time realization. The sharpness of the spectral peaks, combined with the absence of spurious responses, highlights the stability and reliability of the proposed system across different source configurations. Overall, the results confirm that the proposed FPGA-based IMUSIC approach provides high-resolution DOA estimation with excellent accuracy for both moderate and closely spaced source scenarios.

6.1 Root Mean Square Error (RMSE) Performance

Figure 7 illustrates the root mean square error (RMSE) performance of the proposed Improved MUSIC (IMUSIC) algorithm implemented using the Orthogonal–Array architecture as a function of the signal-to-noise ratio (SNR). The performance of the proposed method is compared with conventional MUSIC, Capon beamforming, Root-MUSIC, and the theoretical lower bound represented by the Cramér–Rao Bound (CRB).

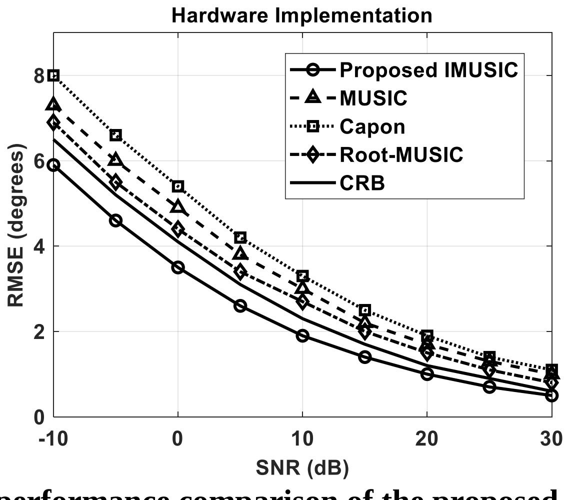

Fig. 7. RMSE versus SNR performance comparison of the proposed IMUSIC algorithm with the Orthogonal–Array against MUSIC, Capon, Root-MUSIC, and the Cramér–Rao Bound (CRB) under hardware-oriented implementation conditions.

DOI: 10.22178/acta.26.1.36

ISSN: 2178-7727

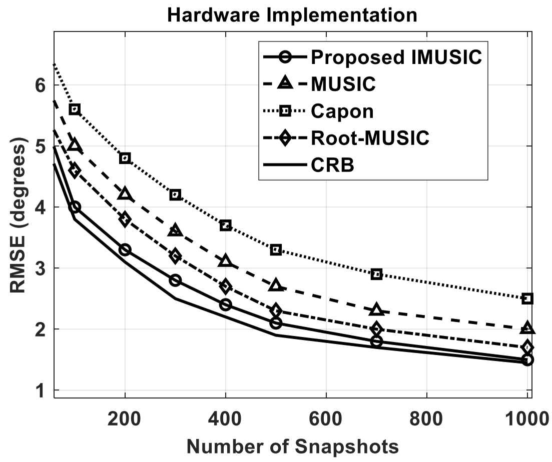

Fig. 8. RMSE performance of the proposed IMUSIC algorithm with the Orthogonal–Array as a function of the number of snapshots, compared with MUSIC, Capon, Root-MUSIC, and the Cramér–Rao Bound (CRB) under hardware-oriented implementation conditions.

As observed from the figure, the RMSE decreases steadily for all algorithms with increasing SNR, indicating improved estimation accuracy as the noise level reduces. Across the entire SNR range, the proposed IMUSIC algorithm with the Orthogonal–Array consistently achieves lower RMSE compared to MUSIC, Capon, and Root-MUSIC, and remains closest to the CRB. This behavior highlights the superior noise robustness and estimation efficiency of the proposed approach under practical operating conditions.

At low SNR values, where estimation is particularly challenging due to noise dominance, the proposed method demonstrates a clear performance advantage. The Orthogonal–Array structure enhances spatial diversity and mitigates the adverse effects of noise and sample imperfections, enabling reliable subspace separation even in noisy environments. In contrast, Capon beamforming shows higher RMSE due to its sensitivity to noise and finite data effects, while conventional MUSIC and Root-MUSIC exhibit moderate improvement but remain less accurate than the proposed method.

At moderate and high SNR levels, the RMSE achieved by the proposed IMUSIC algorithm approaches the CRB, indicating near-optimal estimation performance. This close proximity to the theoretical bound confirms that the proposed Orthogonal–Array-based implementation preserves the desirable characteristics of the IMUSIC algorithm while being suitable for hardware realization.

Figure 8 illustrates the root mean square error (RMSE) performance of the proposed Improved MUSIC (IMUSIC) algorithm implemented using the Orthogonal–Array architecture as the number of snapshots increases. The performance of the proposed method is compared with conventional MUSIC, Capon beamforming, Root-MUSIC, and the theoretical lower bound represented by the Cramér–Rao Bound (CRB). As observed from the figure, the RMSE decreases monotonically for all methods as the number of snapshots increases, which reflects the improved estimation reliability obtained from larger data records. Among the compared techniques, the proposed IMUSIC algorithm with the Orthogonal–Array consistently achieves the lowest RMSE across the entire range of snapshots, remaining closest to the CRB. This behavior demonstrates the superior estimation accuracy and robustness of the proposed approach under limited as well as large snapshot conditions.

The improved performance of the proposed method can be attributed to the Orthogonal–Array structure, which enhances spatial diversity and reduces correlation effects among sensor measurements. This structural advantage enables more accurate subspace separation, leading to sharper spectral peaks and reduced estimation error when compared to conventional array configurations. In contrast, the Capon method exhibits higher RMSE due to its sensitivity to noise and finite sample effects, while conventional MUSIC and Root-MUSIC show moderate improvement with increasing snapshots but remain inferior to the proposed approach.
Another important observation is the stable convergence behavior of the proposed IMUSIC algorithm under

DOI: 10.22178/acta.26.1.36

ISSN: 2178-7727

hardware-oriented constraints. Even at a relatively small number of snapshots, the RMSE achieved by the proposed method is significantly lower than that of the benchmark techniques, indicating its suitability for real-time and resource-constrained implementations such as FPGA-based systems.

CONCLUSION

This work presented an FPGA-based Orthogonal–Array IMUSIC algorithm for accurate and hardware-efficient direction-of-arrival estimation. The proposed Orthogonal–Array structure enhances spatial diversity and improves estimation robustness under noisy and limited-snapshot conditions. Performance evaluation using RMSE analysis demonstrates that the proposed method consistently outperforms conventional MUSIC, Capon, and Root-MUSIC approaches and closely approaches the Cramér–Rao Bound across varying SNR and snapshot scenarios. The obtained results confirm the effectiveness and suitability of the proposed FPGA-oriented IMUSIC architecture for real-time smart antenna, radar, and wireless communication applications.

REFERENCES

1. K. H. Yeap, and A. Khandare, “Sigmoid-enhanced robust adaptive beamforming for sensor arrays,” Signal, Image and Video Processing, vol. 19, no. 4, p. 304, 2025.
2. M. Alagirisamy, S. K. Selvaperumal, N. Ramasendran, and N. T. Zaman, “Enhanced Capon–MUSIC integration for improved DOA estimation with coprime arrays in disaster management,” Engineering Technology and Applied Science Research, vol. 15, no. 2, pp. 20653–20659, 2025.
3. A. Sharma, M. Patil, A. B. M. Valencia, and K. Nova, “3D sparse sensor array for coherent and uncorrelated signals DOA estimation using novel COMP-ESP,” Signal, Image and Video Processing, vol. 19, no. 4, p. 283, 2025.
4. G. N. Basavaraj, B. Ainapure, M. R. Sowmya, and F. Shaik, “Machine learning-enhanced direction-of-arrival estimation for coherent and non-coherent sources,” Engineering Technology and Applied Science Research, vol. 15, no. 2, pp. 20647–20652, 2025.
5. K. S. Shashidhara, K. N. Venu, I. G. Saritha, R. Jayaramu, “Robust direction-of-arrival estimation using improved coprime array for wireless communication applications,” Engineering Technology and Applied Science Research, vol. 15, no. 1, pp. 20285–20290, 2025.
6. M. M. Chalavadi, H. C. S. Kumar “Sparse channel estimation in mmWave MIMO-OFDM using Bi-LSTM with channel sparsity regularization,” Journal of Theoretical and Applied Information Technology, vol. 103, no. 17, pp. 6871–6879, 2025.
7. S. Hugar, J. Baligar, K. M. Vanitha, “A highly independent controlled wide and narrow multiband filter based on a metacell,” IETE Journal of Research, early access, 2025.
8. K. H. Yeap, P. X. Tan, H. K. Lee, and Z. I. Rizman, “Design and analysis of 3-nm strained and conventional FinFETs,” ARPN Journal of Engineering and Applied Sciences, vol. 20, no. 8, pp. 491–496, 2025.
9. D. S. Tan, H. Nisar, K. H. Yeap, and M. Amin, “Lumbar intervertebral disc detection and classification with novel deep learning models,” Journal of King Saud University – Computer and Information Sciences, vol. 36, no. 7, p. 102148, 2024.
10. K. R. Niranjan, I. Malik, K. R. Pedada, and A. Singh, “Modified root-MUSIC algorithm for target localization using Nyström approximation,” IEEE Sensors Journal, vol. 24, no. 8, pp. 13209–13216, 2024.
11. M. V. Galindo, A. B. M. Valencia, K. M. Bindiya, A. Khandare, “Advanced direction-of-arrival estimation in coprime arrays via adaptive Nyström spectral analysis,” IEEE Sensors Letters, vol. 8, no. 2, Art. no. 7001204, 2024.
12. R. S. R., M. C. Parameshwara, “A novel adaptive beamforming technology for mobile communication,” IETE Journal of Research, vol. 70, no. 3, pp. 2204–2211, 2024.
13. M. K. Panda, K. H. Yeap, B. Tripathi, and M. Villagómez-Galindo, “Smart antennas: Revolutionizing connectivity through technology convergence and AI,” in Convergence of Antenna Technologies, Electronics and AI, 2024, pp. 1–21.
14. K. H. Yeap, M. C. Loh, P. C. Teh, “Optimization of receiver optics for radio astronomy,” Applied Computational Electromagnetics Society Journal, vol. 39, no. 11, pp. 1012–1018, 2024.

DOI: 10.22178/acta.26.1.36

ISSN: 2178-7727

15. K. S. Goh, K. H. Yeap and P. C. Teh, “A color correction method to minimize lateral chromatic aberration in spherical lens stacks,” Microwave and Optical Technology Letters, vol. 66, no. 1, Art. no. e34003, 2024.
16. S. Hugar, J. Baligar, and K. M. Vanitha, “Multi-band band-pass filter with independently controlled asymmetric dual-band response based on metacell,” Progress in Electromagnetics Research Letters, vol. 122, pp. 81–86, 2024.
17. K. H. Yeap, H. Nisar, G. N. Basavaraj, and M. V. Galindo, “An overview of techniques and best practices to create intuitive and user-friendly human–machine interfaces,” in Artificial Intelligence and Multimodal Signal Processing in Human Machine Interaction, pp. 63–77, 2024.
18. K. S. Shashidhara, M. Aakaash, A. Kumar, B. D. Parameshachari, “IoT-based smart agriculture monitoring system using web application,” in Lecture Notes in Electrical Engineering, vol. 1105, pp. 171–183, 2024.
19. M. Villagómez-Galindo, A. B. M. Valencia, B. V. Suresh, and S. Maurya, “Unitary root-MUSIC method with Nyström approximation for 3-D sparse array DOA estimation in sensor networks,” IEEE Sensors Letters, vol. 8, no. 10, Art. no. 5504004, 2024.
20. S. Hugar, J. Baligar, and P. Z. Alimovna, “Multiband bandpass filter with asymmetric dual-band response based on metacell,” Microwave and Optical Technology Letters, vol. 65, no. 12, pp. 3126–3132, 2023.
21. K. S. Balamurugan, M. Villagómez-Galindo, M. Patil, and A. Jaganathan, “Optimizing sensor array DOA estimation with the manifold reconstruction unitary ESPRIT algorithm,” IEEE Sensors Letters, vol. 7, no. 12, pp. 1–4, Art. no. 7006804, 2023.
22. B. N. Umesh, A. Khandare, S. Datta, and M. Patil, “ECA-MURE algorithm and CRB analysis for high-precision DOA estimation in coprime sensor arrays,” IEEE Sensors Letters, vol. 7, no. 12, pp. 1–4, Art. no. 5504004, 2023.
23. L. Zhang, M. Nagabushanam, B. Ravindra Babu, and A. Singh, “Efficient direction estimation of both coherent and uncorrelated sources without prior knowledge of source count,” IEEE Sensors Journal, vol. 23, no. 18, pp. 21739–21746, 2023.
24. B. N. Umesh, M. Nagabushanam, and B. Ravindra Babu, “Enhanced direction of arrival estimation via fast sensor array processing,” IEEE Sensors Letters, vol. 7, no. 6, 2023.
25. V. Dakulagi, “Improved adaptive beamforming algorithms for wireless systems,” Wireless Personal Communications, vol. 130, no. 1, pp. 625–633, 2023.
26. R. S. Rekha, M. C. Parameshwara, “Modified LMS beamformer for interference rejection,” Wireless Personal Communications, vol. 129, no. 3, pp. 2199–2211, 2023.
27. R. Dakulagi, K. H. Yeap, and H. Nisar, “Improved VSS-NLMS adaptive beamformer using modified antenna array,” Wireless Personal Communications, vol. 128, no. 4, pp. 2741–2752, 2023.
28. Z. X. Oh, K. H. Yeap, P. C. Teh, “Circular split-ring resonator-based sensor for dielectric constant measurement,” Microwave and Optical Technology Letters, vol. 65, no. 2, pp. 513–518, 2023.
29. V. Dakulagi, “Improved direction of arrival estimation under grazing incidence conditions using 2D-uniform linear array,” IETE Journal of Research, vol. 69, no. 1, pp. 165–172, 2023.
30. K. S. Shashidhara, H. Girish, M. C. Parameshwara, B. K. Rai, “A novel approach for identification of healthy and unhealthy leaves using scale invariant feature transform and shading histogram-PCA techniques,” in Lecture Notes in Electrical Engineering, vol. 928, pp. 549–555, 2023.
31. H. K. Bhaldar, S. K. Gowre, M. S. Mathpati, P. Mankal, “Design of circular microstrip textile antenna for UWB application,” IETE Journal of Research, vol. 69, no. 9, pp. 5951–5964, 2023.
32. M. Mathpati, K. S. Sheshidhara, A. A. Jadhav, and D. Yadav, “A hexagonal Sierpinski fractal antenna for multiband wireless applications,” in Lecture Notes in Electrical Engineering, vol. 928, pp. 189–194, 2023.
33. B. Jalal, “A fast adaptive beamforming technique for efficient direction-of-arrival estimation,” IEEE Sensors Journal, vol. 22, no. 23, pp. 23109–23116, 2022.
34. J. He, and T. Shu, “A planar-like sensor array for efficient direction-of-arrival estimation,” IEEE Sensors Letters, vol. 6, no. 9, Art. no. 7003304, 2022.
35. T. Shu, J. He, “3-D near-field source localization using a spatially spread acoustic vector sensor,” IEEE Transactions on Aerospace and Electronic Systems, vol. 58, no. 1, pp. 180–188, 2022.

DOI: 10.22178/acta.26.1.36

ISSN: 2178-7727

36. M. Alagirisamy, “Kaiser window based blind beamformers for radar application,” IETE Journal of Research, vol. 68, no. 3, pp. 2106–2112, 2022.
37. P. G. Paga, H. C. Nagaraj, K. S. Shashidhara, and K. H. Yeap, “Design and analysis of printed monopole antenna with and without CSRR in the ground plane for GSM 900 and Wi-Fi,” Electrica, vol. 22, no. 1, pp. 92–100, 2022.
38. K. S. Shashidhara, J. Kaur, M. Singh, and R. K. Ratnesh, “A new Kaiser–Bessel constant modulus technique for smart antenna beamforming,” in Lecture Notes in Electrical Engineering, vol. 790, pp. 723–730, 2022.
39. D. S. Tan, D. Mahmood, H. Nisar, and A. Elaraby, “Comparison of segmentation performance of activated sludge flocs using bright-field and phase-contrast microscopy at different magnifications,” IOP Conference Series: Earth and Environmental Science, vol. 945, no. 1, Art. no. 012024, 2021.
40. J. He, T. Shu, and L. Li, “Simultaneous interference localization and array calibration for robust adaptive beamforming with partly calibrated arrays,” IEEE Transactions on Aerospace and Electronic Systems, vol. 57, no. 5, pp. 2850–2863, 2021.
41. M. S. Mathpati, M. Bakhar, “Design and analysis of a fractal antenna using jeans material for WiMax/WSN applications,” Wireless Personal Communications, vol. 119, no. 4, pp. 3517–3527, 2021.
42. P. Mankal, S. C. Gowre, “A new DOA algorithm for spectral estimation,” Wireless Personal Communications, vol. 119, no. 2, pp. 1729–1741, 2021.
43. K. H. Yeap, H. Nisar, “Warpage reduction for power MOSFET wafers,” Electrica, vol. 21, no. 2, pp. 173–179, 2021.
44. V. Dakulagi, “A new approach to achieve a trade-off between direction-of-arrival estimation performance and computational complexity,” IEEE Communications Letters, vol. 25, no. 4, pp. 1183–1186, Art. no. 9310197, 2021.
45. V. Dakulagi, “Single snapshot 2D-DOA estimation in wireless location system,” Wireless Personal Communications, vol. 117, no. 3, pp. 2327–2339, 2021.
46. Jin He, “Improved direction-of-arrival estimation and its implementation for modified symmetric sensor array,” IEEE Sensors Journal, vol. 21, no. 4, pp. 5213–5220, Art. no. 9225069, 2021.
47. P. P. S. Dhaliwal, M. Kumar, “Optimization of serviceability of mobile communication towers under capital constraints,” in Smart Innovation, Systems and Technologies, vol. 225, pp. 431–439, 2021.
48. V. Dakulagi, “Robust modified multiple signal classification algorithm for direction of arrival estimation,” Wireless Personal Communications, vol. 115, no. 3, pp. 2535–2550, 2020.
49. V. Dakulagi, “A new Nyström approximation based efficient coherent DOA estimator for radar applications,” AEU – International Journal of Electronics and Communications, vol. 124, Art. no. 153328, 2020.
50. M. Alagirisamy, and M. Singh, “Efficient coherent direction-of-arrival estimation and realization using digital signal processor,” IEEE Transactions on Antennas and Propagation, vol. 68, no. 9, pp. 6675–6682, Art. no. 9108563, 2020.
51. R. K. Ratnesh, M. Singh, S. Pathak, “Reactive magnetron sputtered–assisted deposition of nanocomposite thin films with tuneable magnetic, electrical and interfacial properties,” Journal of Nanoparticle Research, vol. 22, no. 9, Art. no. 290, 2020.
52. M. Alagirisamy, “Adaptive beamformers for high-speed mobile communication,” Wireless Personal Communications, vol. 113, no. 4, pp. 1691–1707, 2020.
53. K. H. Yeap, W. G. Lim, T. Tang, “Development of a simple home-brew radio telescope,” in Analyzing the Physics of Radio Telescopes and Radio Astronomy, pp. 56–66, 2020.
54. Md. Bakhar, “Advances in smart antenna systems for wireless communication,” Wireless Personal Communications, vol. 110, no. 2, pp. 931–957, 2020.
55. S. Wang, C. Gao, Q. Zhang, J. Cai, and B. Zong, “Research and experiment of radar signal support vector clustering sorting based on feature extraction and feature selection,” IEEE Access, vol. 8, pp. 93322–93334, Art. no. 9090144, 2020.
56. M. Alagirisamy, “Adaptive beamformers using 2D-novel ULA for cellular communication,” SN Applied Sciences, vol. 1, no. 9, Art. no. 1001, 2019.
57. Md. Bakhar, “Smart antenna system for DOA estimation using single snapshot,” Wireless Personal Communications, vol. 107, no. 1, pp. 81–93, 2019.

DOI: 10.22178/acta.26.1.36

ISSN: 2178-7727

58. A. Noubade, A. Agasgere, P. Doddi, and K. Fatima, "Modified adaptive beamforming algorithms for 4G-LTE smart-phones," in Advances in Intelligent Systems and Computing, vol. 898, pp. 561–568, 2019.
59. M. Bakhar, "Efficient blind beamforming algorithms for phased array and MIMO radar," IETE Journal of Research, vol. 64, no. 2, pp. 241–246, 2018.
60. M. Bakhar, "A novel LMS beamformer for adaptive antenna array," Procedia Computer Science, vol. 115, pp. 94–100, 2017.
61. M. Bakhar, and R. M. Vani, "Robust blind beam formers for smart antenna system using window techniques," Procedia Computer Science, vol. 93, pp. 713–720, 2016.
62. M. Bakhar, R. M. Vani, and P. V. Hunagund, "Implementation and optimization of modified MUSIC algorithm for high resolution DOA estimation," in Proc. IEEE MTT-S Int. Microwave and RF Conf. (IMaRC), 2014, pp. 190–193, Art. no. 7038985.

DOI: 10.22178/acta.26.1.36